IET Communications

Research Article

Parallel combinatory multicarrier modulation in underwater acoustic communications

ISSN 1751-8628
Received on 18th April 2016
Revised 30th December 2016
Accepted on 4th March 2017
E-First on 26th June 2017
doi: 10.1049/iet-com.2016.0475
www.ietdl.org

Qin Lu[1], Xiaoyi Hu[2], Deqing Wang[2], Shengli Zhou[1] ✉

[1]*Department of Electrical and Computer Engineering, University of Connecticut, Storrs, CT 06269, USA*
[2]*Key Laboratory of Underwater Acoustic Communication and Marine Information Technology, Xiamen University, Xiamen 361005, People's Republic of China*
✉ *E-mail: shengli.zhou@uconn.edu*

Abstract: Parallel combinatory multicarrier (PCMC) modulation is a generalisation of the legacy multicarrier frequency shift keying (FSK) scheme, where for each group of M subcarriers, more than one (say L) subcarriers are chosen for simultaneous transmission. The PCMC scheme provides an effective way to increase the spectral efficiency while maintaining non-coherent detection at the receiver. This study provides an in-depth study of the PCMC scheme with emphasis on how to couple with binary or non-binary channel coding. One favourable system configuration is identified, having parameters $(L,M) = (4,8)$, which increases the spectral efficiency by 50% relative to the most efficient FSK scheme from the FSK family. Coupled with non-binary low-density parity-check (LDPC) coding over the Galois field GF(64), the PCMC scheme with $(L,M) = (4,8)$ is shown to have robust performance in multipath fading channels.

1 Introduction

Underwater acoustic communications and networks have been actively studied in recent years, see, e.g. [1, 2] and references therein, and also example references from the Institution of Engineering and Technology (IET) journals [3–10]. On parallel-to-single-carrier transmissions, various forms of multicarrier modulation have been pursued for underwater acoustic communications [11, 12]. On the basis of the receiver processing mechanism, underwater multicarrier schemes which can be broadly divided into the following categories:

- *Non-coherent detection*: Multicarrier frequency shift keying (MFSK) is one legacy scheme with low-complexity non-coherent detection at the receiver, where one out of each group of M subcarriers is selected for transmission to carry $\log_2 M$ bits of information [13–16]. The spectral efficiency of multicarrier MFSK is 0.5 bits per subcarrier for 2-FSK and 4-FSK, and 0.25 bits per subcarrier for 16-FSK, and further reduces when M increases.

  On each subcarrier of an orthogonal frequency division multiplexing (OFDM) symbol, on–off keying has been applied to have a spectral efficiency of 1 bit per subcarrier [17]. However, a different energy threshold is needed on each subcarrier for non-coherent detection, and threshold tuning becomes a challenging task at the receiver.
- *Differential detection:* Differential M-ary phase shift keying (PSK) can be applied across time or frequency in underwater OFDM-based systems [18, 19], having a spectrum efficiency of $\log_2 M$ bits per subcarrier. The performance of a differential scheme depends on the channel coherence across time or frequency.
- *Coherent detection:* Coherent modulations such as PSK and quadrature amplitude modulation (QAM) can be applied in underwater OFDM systems, where channel estimation is one integral module of a coherent receiver [11, 20, 21]. For a PSK or QAM constellation with size M, the spectral efficiency is $\log_2 M$ per subcarrier. Through parallel transmissions from multiple transmitters, multi-input–multi-output OFDM can further increase the spectral efficiency substantially [22, 23].

This paper deals with the parallel combinatory (PC) multicarrier modulation for underwater acoustic communications. The PC concept was conceived in [24] for a direct sequence spread spectrum system where multiple sequences are selected for parallel transmissions. The application of the PC concept in multicarrier underwater acoustic communications was done in [25]. The PC multicarrier (PCMC) scheme can be viewed as a generalisation of the legacy multicarrier MFSK modulation for underwater acoustic systems [13, 14, 16]. For a group of M subcarriers, instead of one subcarrier was used as in the MFSK scheme, multiple (say L) subcarriers are chosen for simultaneous transmission. When $L = 1$, it reduces to MFSK. By properly choosing a large L, the spectral efficiency of the PCMC scheme can increase from 0.5 bits per subcarrier to 1 bit per subcarrier, while maintaining low-complexity non-coherent detection at the receiver.

Only uncoded PCMC transmissions have been treated in [25]. In this paper, we further explore this scheme and provide an in-depth study of a coded PCMC system. Our focus is on how the receiver computes the soft information as needed by a binary or non-binary decoder, without a need to estimate the signal and noise variances. Numerical results reveal several interesting findings:

- First, the coupling of PCMC with a binary code such as the convolutional code has poor performance in Rayleigh fading channels, while the coupling of PCMC with a non-binary code has robust performance by avoiding the potential loss due to bit and frequency conversion. This performance difference is rather drastic for the PCMC modulation, unlike the case with coherent PSK/QAM modulations as studied in [26].
- Second, out of the PCMC family, we have identified one favourable configuration having parameters $(L,M) = (4,8)$, which has a spectral efficiency of 0.75 bits per subcarrier, 50% higher than the 4-FSK scheme. A side-by-side comparison shows that the (4,8) PCMC scheme combined with rate 1/2 coding outperforms the legacy multicarrier 4-FSK scheme combined with rate 3/4 coding, both of them having the same data rate. This shows that the PCMC scheme is one appealing choice for a practical underwater acoustic system with non-coherent detection.

The results herein developed in the context of underwater acoustic communications are directly applicable to radio communications.

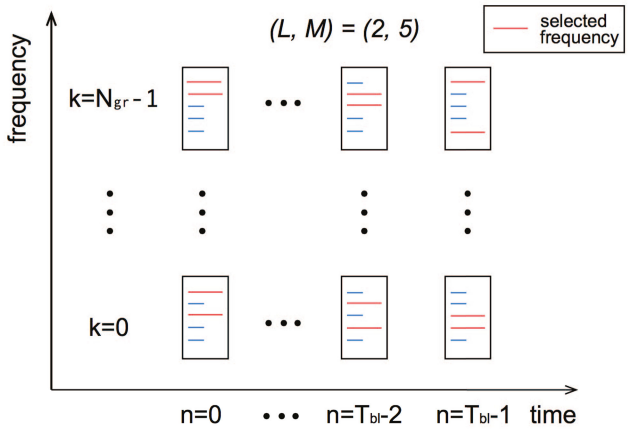

Fig. 1 *Illustration of one coded packet based on the PCMC modulation*

However, underwater acoustic channels have fast variations in addition to the large delay spread, phase-coherent communications are far more challenging than in radio channels [1, 11, 12]. The work in this paper is hence especially appealing to underwater acoustic applications where low-complexity non-coherent receivers might be preferred.

The rest of this paper is organised as follows. The transmitter and receiver are described in Sections 2 and 3, respectively. Simulation results are presented in Section 4 and conclusions are drawn in Section 5.

2 Transmitter design

Consider one data packet that can span multiple data blocks, say N_{bl} data blocks, as depicted in Fig. 1. Each block uses a multicarrier format with K_{d} active subcarriers, where the subcarriers could be non-overlapping as in frequency division multiplexing or the subcarriers could be overlapping as in OFDM. To use the (L,M) PC scheme, K_{d} active subcarriers are divided into N_{gr} groups, so that $K_{\text{d}} = N_{\text{gr}}M$. Each group of M subcarriers carries

$$q = \lfloor \log_2 C_M^L \rfloor \tag{1}$$

bits, where $\lfloor \cdot \rfloor$ is the floor operation. Consider a channel coding with rate r_{c}, each data packet contains $N_{\text{bl}}N_{\text{gr}}qr_{\text{c}}$ information bits.

The coding and modulation process in the PCMC scheme is as follows. First, consider a binary encoder. The bit sequence $b[n]$ is encoded and interleaved to obtain the $c[n]$. Those $N_{\text{bl}}N_{\text{gr}}q$ coded bits are divided into $N_{\text{bl}}N_{\text{gr}}$ segments. The coded bits assigned to the kth group of the nth block are denoted as

$$\{c_{n,k}[0], \ldots, c_{n,k}[q-1]\} \tag{2}$$

based on which a decimal value can be obtained as

$$d_{n,k} = \sum_{l=0}^{q-1} c_{n,k}[l]\, 2^l \tag{3}$$

For a non-binary encoder, $N_{\text{bl}}N_{\text{gr}}r_{\text{c}}$ information symbols over Galois field GF(Q), where $Q = 2^q$, are encoded into $N_{\text{bl}}N_{\text{gr}}$ coded symbols [26]. For each coded symbol, a decimal value $d_{n,k}$ can be assigned from 0 to $Q-1$.

The mapping of the decimal value $d_{n,k}$ to the subcarrier frequencies is done through a look up table. For the kth group at the nth block, define the corresponding M subcarriers in

$$\{f_{n,k}[0], \ldots, f_{n,k}[M-1]\} \tag{4}$$

where the subcarriers might be different for different blocks, corresponding to a frequency-hopped system. Define a selection matrix $\boldsymbol{A}$ of size $Q \times M$, where each entry takes the value of either 0 or 1, and the sum of each row equals L. When $d_{n,k} = i$, the ith row of the selection matrix $\boldsymbol{A}$ is used to select L out of M subcarriers for transmission corresponding to those entries $A[i,j] = 1$, $j = 0, \ldots, M-1$. The rules for constructing the selection matrix are discussed in [25]. For example, if $(L,M) = (2,5)$, we have $q = \log_2 Q = \lfloor \log_2 C_5^2 \rfloor = 3$, and an example 8×5 selection matrix is

$$\boldsymbol{A} = \begin{bmatrix} 1 & 1 & 0 & 0 & 0 \\ 1 & 0 & 1 & 0 & 0 \\ 1 & 0 & 0 & 1 & 0 \\ 1 & 0 & 0 & 0 & 1 \\ 0 & 1 & 1 & 0 & 0 \\ 0 & 1 & 0 & 1 & 0 \\ 0 & 1 & 0 & 0 & 1 \\ 0 & 0 & 1 & 1 & 0 \end{bmatrix} \tag{5}$$

Assume that each subcarrier occupies a time duration T. Between consecutive symbols, a guard interval of duration T_{g} is inserted to avoid inter block interference. Thus each block has duration $T_{\text{bl}} = T + T_{\text{g}}$. Define a rectangular window as

$$g(t) = \begin{cases} 1, & t \in [0, T] \\ 0, & \text{otherwise} \end{cases} \tag{6}$$

The transmitted passband signal for the nth block is

$$\tilde{x}_n(t) = \text{Re}\left\{ \sum_{k=0}^{N_{\text{gr}}-1} \sum_{j=0}^{M-1} A[d_{n,k}, j] e^{\text{j}\phi_{n,i}[j]} e^{\text{j}2\pi f_{n,k}[j]t} g(t - nT_{\text{bl}}) \right\}, \quad t \in [nT_{\text{bl}}, nT_{\text{bl}} + T_{\text{bl}}) \tag{7}$$

The phase shifts $e^{\phi_{n,k}[i]}$ are used to control the peak-to-power ratio of the transmitted signal [16]. They can be randomly generated, and a good set is chosen following the selective mapping method based on random search [27–29].

3 Receiver design

Underwater acoustic channels are often time-varying, and proper Doppler compensation needs to be carried out before demodulation. The Doppler shift compensation method in [16] for multicarrier MFSK can be applied to the PCMC scheme after slight modification, which however, is not the focus of this paper. Assume that after proper Doppler compensation, the channel within each block can be viewed as static, but could be different from block to block. Within a block, one can characterise the static channel as a multipath channel with an impulse response as

$$h(\tau) = \sum_{p=1}^{N_{\text{pa}}} A_p \delta(\tau - \tau_p) \tag{8}$$

where N_{pa} denotes the number of paths and A_p, τ_p, respectively, represent the amplitude and initial delay of the pth path.

After passing through the channel as specified in (8), the received signal at the nth block is

$$\tilde{y}_n(t) = \sum_{p=1}^{N_{\text{pa}}} A_p \tilde{x}_n(t - \tau_p) + \tilde{w}_n(t) \tag{9}$$

where $\tilde{x}_n(t)$ is the transmitted passband signal in (7) and $\tilde{w}_n(t)$ is additive noise. The frequency-domain samples on M subcarriers of the kth group are obtained as

$$z_{n,k}[m] = \int_{nT_{\mathrm{bl}}}^{nT_{\mathrm{bl}}+T_{\mathrm{ch}}} \tilde{y}_n(t) \mathrm{e}^{-\mathrm{j}2\pi f_{n,k}[m]t} \mathrm{d}t \tag{10}$$

where T_{ch} is the maximum channel delay. The squared amplitude is obtained as

$$Z_{n,k}[m] = |z_{n,k}[m]|^2 \tag{11}$$

The detection for the kth group of the nth block is done based on the M samples $\{Z_{n,k}[m]\}_{m=0}^{M-1}$.

3.1 Likelihood function under Rayleigh fading

Decoding for each group is done separately, and now consider one group of samples $\{Z_{n,k}[m]\}_{m=0}^{M-1}$. For brevity, drop the indices n,k, and denote the set of samples as $\{Z[m]\}_{m=0}^{M-1}$. Assuming that the channel frequency response on each subcarrier is Rayleigh distributed, the probability distribution of $Z[m]$ as conditioned on $d = i$ is [30]

$$f(Z[m]|d=i) = \begin{cases} \dfrac{1}{\sigma_w^2}\exp\left(-\dfrac{Z[m]}{\sigma_{\mathrm{w}}^2}\right), & \text{if } A[i,m]=0 \\ \dfrac{1}{\sigma_{\mathrm{s}}^2+\sigma_{\mathrm{w}}^2}\exp\left(-\dfrac{Z[m]}{\sigma_{\mathrm{s}}^2+\sigma_{\mathrm{w}}^2}\right), & \text{if } A[i,m]=1 \end{cases} \tag{12}$$

where σ_{s}^2 and σ_{w}^2 are the signal and noise variances, respectively. The log-likelihood function of all the M observations as conditioned on $d = i$ is

$$\begin{aligned} &\ln f(\{Z[m]\}_{m=0}^{M-1}|d=i) \\ &= \sum_{m=0}^{M-1} A[i,m]\frac{-Z[m]}{\sigma_{\mathrm{s}}^2+\sigma_{\mathrm{w}}^2} + \sum_{m=0}^{M-1}(1-A[i,m])\frac{-Z[m]}{\sigma_{\mathrm{w}}^2} + C_1 \\ &= \sum_{m=0}^{M-1} A[i,m]\frac{Z[m]\sigma_{\mathrm{s}}^2}{\sigma_w^2(\sigma_{\mathrm{s}}^2+\sigma_{\mathrm{w}}^2)} + C_2 \end{aligned} \tag{13}$$

where C_1, C_2 are constants irrelevant to the detection.

3.2 Binary decoding

A binary decoder requires the log-likelihood ratio (LLR) of each bit from the demodulator. The LLR for $b[l]$ is defined as

$$\mathrm{LLR}(b[l]) = \ln\frac{P\left(b[l]=1|\{Z[m]\}_{m=0}^{M-1}\right)}{P\left(b[l]=0|\{Z[m]\}_{m=0}^{M-1}\right)} \tag{14}$$

With the likelihood function in (12), the following LLR expression is obtained [30]:

$$\begin{aligned} &\mathrm{LLR}(b[l]) = \ln \\ &\left(\frac{\sum_{\{i;b[l]=1\}}\exp\left(\sum_{m=0}^{M-1}A[i,m]((Z[m]\sigma_{\mathrm{s}}^2)/(\sigma_w^2(\sigma_{\mathrm{s}}^2+\sigma_{\mathrm{w}}^2)))\right)}{\sum_{\{i;b[l]=0\}}\exp\left(\prod_{m=0}^{M-1}A[i,m]((Z[m]\sigma_{\mathrm{s}}^2)/(\sigma_w^2(\sigma_{\mathrm{s}}^2+\sigma_{\mathrm{w}}^2)))\right)}\right) \end{aligned} \tag{15}$$

Here, we adopt the max-log approximation, $\ln(\mathrm{e}^x + \mathrm{e}^y) \simeq \max(x, y)$, to obtain (see (16)) This way, estimation of the signal and noise variances is not needed. Following the choices in [26], binary convolutional code is used in our numerical study, and the Viterbi algorithm is used for decoding [31].

3.3 Non-binary decoding

For non-binary coding, each coded symbol over GF(Q) is mapped to one (L,M) symbol. The non-binary decoder needs the LLR-vector as

$$\boldsymbol{L} = [L_0, L_1, \ldots, L_{Q-1}] \tag{17}$$

where

$$L_i = \ln\frac{P\left(d=i|\{Z[m]\}_{m=0}^{M-1}\right)}{P\left(d=0|\{Z[m]\}_{m=0}^{M-1}\right)} \tag{18}$$

Unlike the binary case, the LLR for all the symbols are enumerated, and hence bit-to-symbol mapping at the modulation level becomes not important [26]. With the likelihood function in (12), we obtain

$$L_i = \sum_{m=1}^{M} A[i,m]\frac{Z[m]\sigma_{\mathrm{s}}^2}{\sigma_{\mathrm{w}}^2(\sigma_{\mathrm{s}}^2+\sigma_{\mathrm{w}}^2)} - \sum_{m=1}^{M} A[0,m]\frac{Z[m]\sigma_{\mathrm{s}}^2}{\sigma_{\mathrm{w}}^2(\sigma_{\mathrm{s}}^2+\sigma_w^2)} \tag{19}$$

To avoid the need of the estimation of the signal and the noise variances, one can scale L_i as

$$L_i \propto \sum_{m=1}^{M} A[i,m]Z[m] - \sum_{m=1}^{M} A[0,m]Z[m] \tag{20}$$

Following the choices in [26], non-binary LDPC codes are used in our numerical study, and the min-sum algorithm is used for non-binary LDPC decoding.

4 Numerical results

Table 1 lists the spectral efficiency for the MFSK scheme when the number of bits per FSK symbol increases from 1 to 8. The maximum spectral efficiency within the MFSK family is 0.5 when 2-FSK or 4-FSK is used. The spectral efficiency decreases toward to zero as M increases. For the PC scheme, we fix the number of active subcarriers L and do a grid search on the total number of subcarriers M to obtain the largest spectral efficiency. Table 2 summarises the best spectral efficiency when L increases from 1 to 8. Clearly, the relationship among the parameters $\{M,L,q\}$ in Table 2 for the PC scheme is different from that in Table 1 for the MFSK scheme. For the PC scheme, the maximum spectral efficiency increases as L increases, and can approach 1 as both L and M become large.

With the same bit energy, the symbol energy is $E_{\mathrm{s}} = qE_{\mathrm{b}}/L$. The bigger q/L, the better accumulation of the energy on each active subcarrier, which might lead to better performance. This is why 4-FSK has a much better performance than 2-FSK while both of them have the same efficiency [31]. Another note is the configuration of $(L,M) = (3,6)$ and $q = 4$, which is of interest as it can match well with a non-binary code over GF(16). However, $q/L = 1.33$ for the (3,6) case, less than $q/L = 1.66$ for the (3,7) case, and hence the (3,6) case is less power efficient.

For performance illustration, we will use the (1,4), (2,5), and (4,8) configurations next.

4.1 Baseband additive white Gaussian noise (AWGN) and independent and identically distributed (i.i.d.) fading channels

We consider a baseband equivalent channel model first. On each subcarrier, the channel output is related to the channel input as

$$z[k] = \begin{cases} H[k] + w[k], & \text{signal present} \\ w[k], & \text{signal absent} \end{cases} \tag{21}$$

$$\mathrm{LLR}(b[l]) \propto \max_{\{i;b[l]=1\}} \sum_{m=0}^{M-1} A[i,m]Z[i] - \max_{\{i;b[l]=0\}} \sum_{m=0}^{M-1} A[i,m]Z[i] \tag{16}$$

Table 1 Spectral efficiency for *M*-ary FSK, where $q = \log_2 M$

L	1	1	1	1	1	1	1	1
M	2	4	8	16	32	64	128	256
Q	1	2	3	4	5	6	7	8
$\frac{q}{M}$	0.50	0.50	0.37	0.25	0.16	0.09	0.05	0.03

Table 2 Spectral efficiency for (L, M) PC, where $q = \lfloor \log_2 C_M^L \rfloor$

L	1	2	3	4	5	6	7	8
M	4	5	7	8	13	15	17	19
q	2	3	5	6	10	12	14	16
$\frac{q}{M}$	0.50	0.60	0.71	0.75	0.77	0.80	0.82	0.84

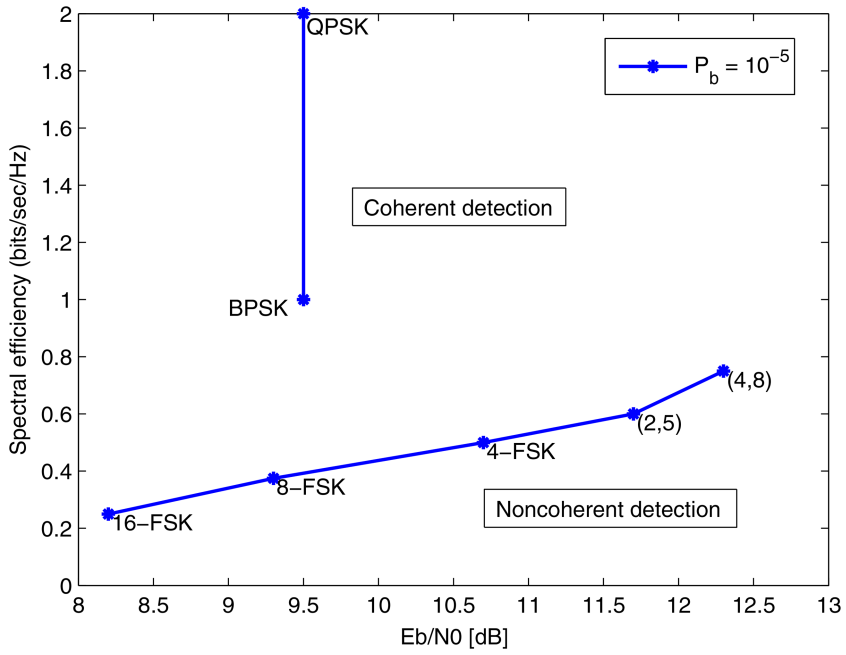

Fig. 2 *Comparison of uncoded digital communication schemes over AWGN*

The noise $w[k]$ is white Gaussian with variance σ_w^2. When $|H[k]| = \sigma_s$, $\forall k$, the channel model corresponds to an AWGN channel. When $H[k]$ is complex Gaussian with variance $H[k] \sim \mathcal{CN}(0, \sigma_s^2)$ and the channels are uncorrelated across subcarriers, the channel model corresponds to an i.i.d. Rayleigh fading channel.

With the (L,M) configuration, the bit energy-to-noise ratio for an uncoded transmission is defined as

$$\frac{E_b}{N_0} = \frac{L}{q} \cdot \frac{\sigma_s^2}{\sigma_w^2} \tag{22}$$

Fig. 2 shows the needed E_b/N_0 at the bit error rate (BER) of 10^{-5}. Note that Figure 4.6-1 of [31] provides a comparison of many modulation choices, but missed the (1,4), (2,5), and (4,8) points as shown in Fig. 2.

When a rate-r_c channel code is used, the bit energy-to-noise ratio becomes

$$\frac{E_b}{N_0} = \frac{1}{r_c} \cdot \frac{L}{q} \cdot \frac{\sigma_s^2}{\sigma_w^2} \tag{23}$$

The non-binary LDPC codes from [26] are adopted here, where each coded symbol is mapped to one (L,M) symbol. Specifically:

- For the (1,4) case, the rate-(1/2) code over GF(4) is used with the parity-check matrix of size (336,672). The number of information bits is 672.
- For the (2,5) case, the rate-(1/2) code over GF(8) is used with the parity-check matrix of size (336,672). The number of information bits is 1008.
- For the (4,8) case, the rate-(1/2) code over GF(64) is used with the parity-check matrix of size (336,672). The number of information bits is 2016.

For the binary coding, we use the 64-state rate-(1/2) convolutional code with the generator (133,171) [26]. In each case, the number of information bits is chosen to be the same as with non-binary coding.

The BER results for the AWGN and Rayleigh fading channels are reported in Figs. 3 and 4, respectively. One critical observation is that the binary convolutional code is not suitable for the (L,M) modulation, especially the performance is rather poor in Rayleigh fading channels. Non-binary coding avoids the need of bit-to-frequency mapping and vice versa, and achieves robust BER performance when coupled with non-coherent detection in non-faded and fading channels. The advantage of non-binary coding relative to binary coding is much less pronounced when coherent PSK/QAM modulations are used as studied in [26].

The coded BER of the (4,8) configuration catches up with that of (2,5), partly due to a longer (stronger) channel code and partly due to a larger q/L ratio. The (1,4), (2,5), and (4,8) can match well non-binary codes with suitable sizes [26], and are thus interesting

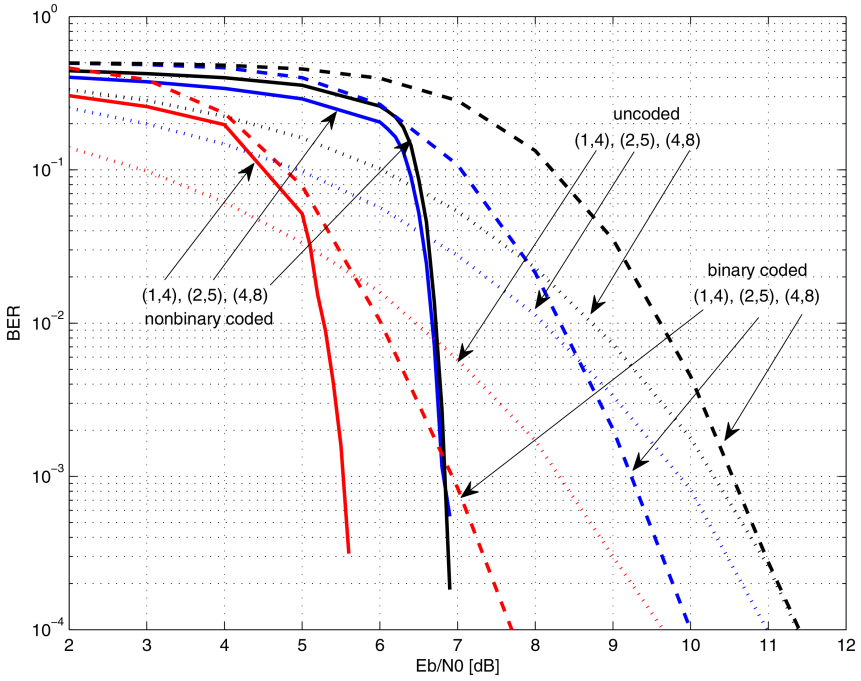

Fig. 3 *BER performance in the baseband AWGN channel*

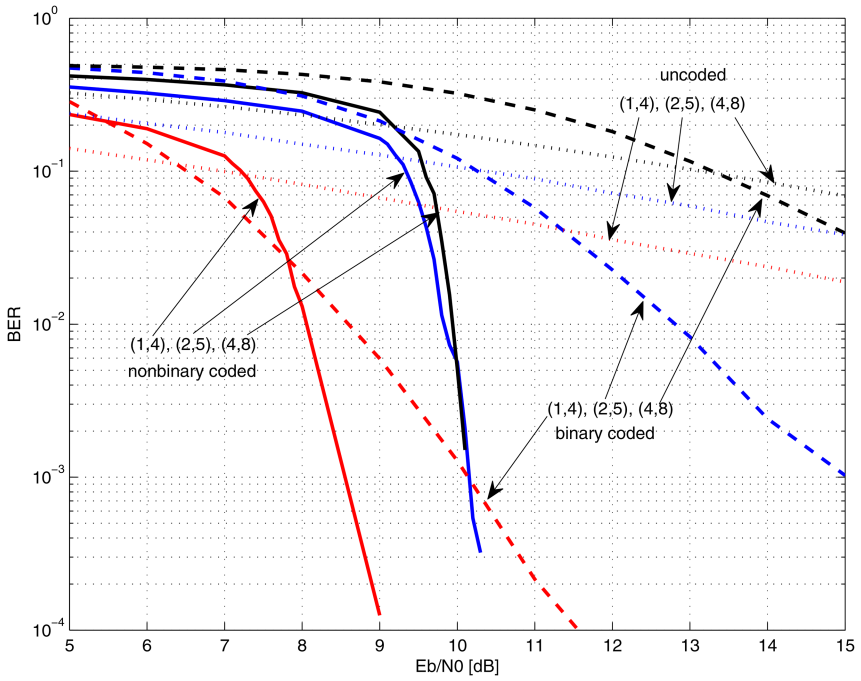

Fig. 4 *BER performance in the baseband Rayleigh fading channel*

for practical use. Further increase of L and M to improve the spectral efficiency might not be suitable for practical implementation due to the complexity increase of non-binary coding in a large GF.

4.2 Passband multipath channels

We now follow the system parameters in [16] to construct a PC-based OFDM system. Assume that there are a total of $K = 1024$ OFDM subcarriers within a total bandwidth of $B = 6$ kHz; hence, the subcarrier spacing is $B/K = 5.86$ Hz and the OFDM symbol duration is $T = K/B = 170.7$ ms. The carrier frequency f_c can be shifted to match with the transducer used in a practical system, but is set to be $f_c = 17$ kHz [16]. Only the middle $K_d = 672$ subcarriers are used, and hence effectively the signal bandwidth is only 3.94 kHz. The guard time between OFDM symbols is chosen $T_g = 79.3$ ms [16]. We consider the following three cases:

- (1,4) coupled with rate-(1/2) LDPC coding with the parity-check matrix (336,672). Each OFDM block has $N_{gr} = 168$ 4-FSK symbols, and one data packet consists of four OFDM blocks. The data rate is

$$R_1 = \frac{672 \cdot 2 \cdot (1/2)}{4(T + T_g)} = 672 \text{ bps} \tag{24}$$

- (1,4) coupled with rate-(3/4) LDPC coding with the parity-check matrix of size (168, 672). Each OFDM block has $N_{gr} = 168$ 4-FSK symbols, and one data packet consists of four OFDM blocks. Owing to the coding rate increase, the data rate is now

$$R_2 = \frac{672 \times 2 \times (3/4)}{4(T + T_g)} = 1008 \text{ bps} \tag{25}$$

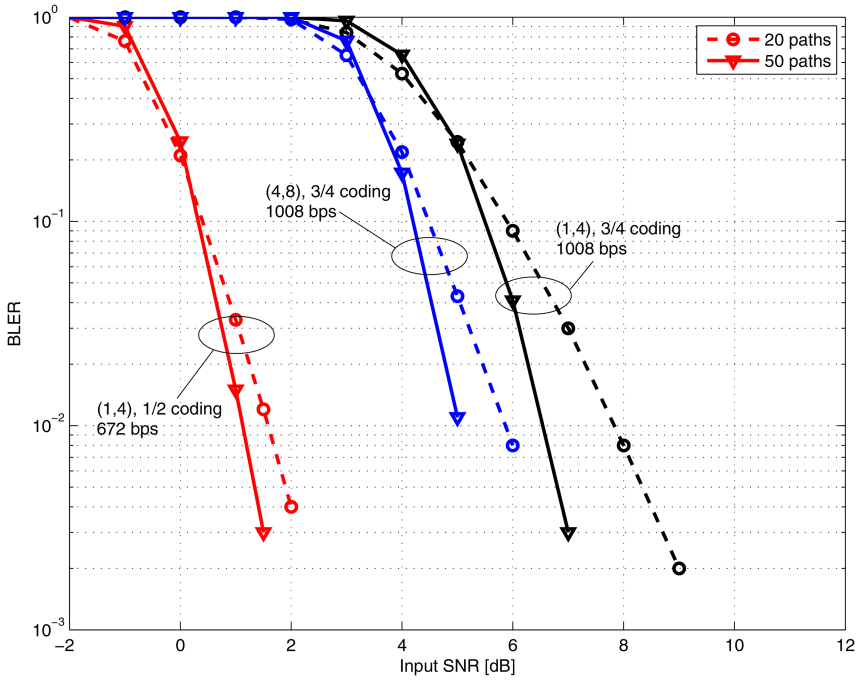

Fig. 5 *Comparison of coded BLER in passband multipath channels*

- (4,8) coupled with rate-1/2 LDPC coding with the parity-check matrix of size (336, 672). Each OFDM block now has $N_{gr} = 84$ (4,8) blocks, and the data packet consists of eight OFDM blocks. The data rate is

$$R_3 = \frac{672 \times 6 \times (1/2)}{8(T + T_g)} = 1008 \text{ bps} \tag{26}$$

The first case with 4-FSK and rate-1/2 coding has been thoroughly tested in [16] using simulations and experimental data, and hence serves a good baseline. The last two cases are of particular interest in this paper. Both of them have identical data rates, but with different modulation and coding choices.

Passband data packets are generated with a sampling rate $f_s = 48$ kHz. The data packets pass through a static multipath channel as defined in (8). The inter-arrival-time of the propagation paths follows an exponential distribution with a mean of 1 ms. The amplitudes of paths are Gaussian distributed with the average power decreasing exponentially with the delay, where the difference between the beginning and the end of the guard time is 20 dB [16]. To be consistent with [16], the input signal-to-noise ratio (SNR) is defined over the 6 kHz frequency band as

$$\text{input SNR} = \frac{\text{signal power within the 6 kHz signal band}}{\text{noise power within the 6 kHz signal band}} \tag{27}$$

The relationship of the SNR and the conventional E_b/N_0 can be related as

$$\text{input SNR} = \frac{K_d}{K} \cdot \frac{q}{M} \cdot r_c \cdot \frac{E_b}{N_0} \tag{28}$$

Fig. 5 shows the packet error rates for two channel settings: (i) fading channels with $N_{pa} = 20$ paths and (ii) fading channels with $N_{pa} = 50$ paths. The block error rate (BLER) performance in the latter setting is better than the former setting, thanks to the increased frequency diversity from more propagation paths. The (1,4) case with rate 1/2 coding has the best performance out of the three systems, but operating at a low data rate of 672 bps. Operating at the same data rate of 1008 bps, the scheme with (4,8) with rate 1/2 coding outperforms the scheme with (1,4) and rate 3/4 coding in multipath fading channels, where the SNR gain is about 1.5 dB at BLER of 10^{-2}. This confirms the practical merit of the PCMC approach relative to the legacy multicarrier MFSK when there is a desire to increase the data rate while still maintaining non-coherent detection.

5 Conclusion

This paper provided a study of a coded PCMC modulation for underwater acoustic communications, where the emphasis is on how to generate the soft information needed by the binary and non-binary decoders. Simulation results reveal that the PCMC scheme coupled with non-binary LDPC coding has robust performance while it is not the case with binary convolutional coding. The non-binary coded (4,8) PCMC scheme was shown to be one favourable choice, which increases the spectrum efficiency while maintaining non-coherent detection at the receiver and robust performance in fading channels.

6 Acknowledgments

The work of X.-Y. Hu was partly supported by the China Scholarship Council under no. 201208350060. The work of D.-Q. Wang was partly supported by the National Natural Science Foundation of China under grant no. 61301098.

7 References

[1] Kilfoyle, D.B., Baggeroer, A.B.: 'The state of the art in underwater acoustic telemetry', *IEEE J. Ocean. Eng.*, 2000, **25**, (1), pp. 4–27

[2] Baggeroer, A.B.: 'An overview of acoustic communications from 2000–2012'. Proc. of the Workshop on Underwater Communications: Channel Modelling Validation, Italy, September 2012

[3] Konstantakos, D.P., Adams, A.E., Sharif, B.S.: 'Multicarrier code division multiple access (MC-CDMA) technique for underwater acoustic communication networks using short spreading sequences', *IEE Proc., Radar Sonar Navig.*, 2004, **151**, (4), pp. 231–239

[4] Konstantakos, D.P., Tsimenidis, C.C., Adams, A.E., *et al.*: 'Comparison of DS-CDMA and MC-CDMA techniques for dual-dispersive fading acoustic communication networks', *IEE Proc., Commun.*, 2005, **152**, (6), pp. 1031–1038

[5] Jamshidi, A.: 'Direct sequence spread spectrum point-to-point communication scheme in underwater acoustic sparse channels', *IET Commun.*, 2011, **5**, (4), pp. 456–466

[6] Qi, C., Wang, X., Wu, L.: 'Underwater acoustic channel estimation based on sparse recovery algorithms', *IET Signal Process..*, 2011, **5**, (8), pp. 739–747

[7] Misra, S., Dash, S., Khatua, M., *et al.*: 'Jamming in underwater sensor networks: detection and mitigation', *IET Commun.*, 2012, **6**, (14), pp. 2178–2188

[8] Wang, P., Zhang, L., Li, V.: 'Asynchronous cooperative transmission for three-dimensional underwater acoustic networks', *IET Commun..*, 2013, **7**, (4), pp. 286–294

[9] Kim, J., Koh, I., Lee, Y.: 'Short-term fading model for signals reflected by ocean surfaces in underwater acoustic communication', *IET Commun.*, 2014, **9**, (9), pp. 1147–1753
[10] Zhang, Y., Liu, L., Sun, D.*, et al.*: 'Single-carrier underwater acoustic communication combined with channel shortening and dichotomous coordinate descent recursive least squares with variable forgetting factor', *IET Commun.*, 2015, **9**, (15), pp. 1867–1876
[11] Zhou, S., Wang, Z.-H.: '*OFDM for underwater acoustic communications*' (John Wiley & Sons, Inc., Chichester, UK, 2014)
[12] Kumar, P., Trivedi, V.K., Kumar, P.: 'Recent trends in multicarrier underwater acoustic communications'. Proc. of IEEE Underwater Technology, Chennai, February 2015
[13] Catipovic, J., Deffenbaugh, M., Freitag, L.*, et al.*: 'An acoustic telemetry system for deep ocean mooring data acquisition and control'. Proc. of MTS/IEEE OCEANS Conf., Seattle, September 1989, pp. 887–892
[14] Scussel, K.F., Rice, J.A., Merriam, S.: 'A new MFSK acoustic modem for operation in adverse underwater channels'. Proc. of MTS/IEEE OCEANS Conf., Halifax, Nova Scotia, October 1997, pp. 247–254
[15] Green, D., Rice, J.A.: 'Channel-tolerant FH-MFSK acoustic signaling for undersea communications and networks', *IEEE J. Ocean. Eng.*, 2000, **25**, (1), pp. 28–39
[16] Cai, X., Wan, L., Huang, Y.*, et al.*: 'Further results on multicarrier MFSK based underwater acoustic communications', *Elsevier J. Phys. Commun.*, 2016, **18**, (1), pp. 15–27
[17] Gendron, P.J.: 'Orthogonal frequency division multiplexing with on–off-keying: noncoherent performance bounds, receiver design and experimental results', *U.S. Navy J. Underwater Acoust.*, 2006, **56**, (2), pp. 267–300
[18] Qu, F., Yang, L.: 'Orthogonal space–time block-differential modulation over underwater acoustic channels'. Proc. of MTS/IEEE OCEANS Conf., Vancouver, BC, 29 September–4 October 2007
[19] Aval, Y.M., Stojanovic, M.: 'Differentially coherent multichannel detection of acoustic OFDM signals', *IEEE J. Ocean. Eng.*, 2015, **40**, (2), pp. 251–268
[20] Li, B., Zhou, S., Stojanovic, M.*, et al.*: 'Multicarrier communication over underwater acoustic channels with nonuniform Doppler shifts', *IEEE J. Ocean. Eng.*, 2008, **33**, (2), pp. 198–209
[21] Lu, Q., Huang, Y., Wang, Z.-H.*, et al.*: 'Characterization and receiver design for underwater acoustic channels with large Doppler spread'. Proc. of IEEE/MTS OCEANS Conf., Washington, DC, October 2015
[22] Li, B., Huang, J., Zhou, S.*, et al.*: 'MIMO-OFDM for high rate underwater acoustic communications', *IEEE J. Ocean. Eng.*, 2009, **34**, (4), pp. 634–644
[23] Ceballos, P., Stojanovic, M.: 'Adaptive channel estimation and data detection for underwater acoustic MIMO OFDM systems', *IEEE J. Ocean. Eng.*, 2010, **35**, (3), pp. 635–646
[24] Sasaki, S., Kikuchi, H., Zhu, J.*, et al.*: 'Multiple access performance of parallel combinatory spread spectrum communication systems in nonfading and Rayleigh fading channels', *IEICE Trans. Commun.*, **78**, (8), pp. 1152–1161
[25] Zhan, C., Xu, F., Hu, X.: 'Parallel combinatory multicarrier frequency-hopped spread spectrum for long range and shallow underwater acoustic communications'. Proc. of MTS/IEEE OCEANS, Bergen, June 2013
[26] Huang, J., Zhou, S., Willett, P.: 'Nonbinary LDPC coding for multicarrier underwater acoustic communication', *IEEE J. Sel. Areas Commun.*, 2008, **26**, (9), pp. 1684–1696
[27] Mestdagh, D., Spruyt, P.: 'A method to reduce the probability of clipping in DMT-based transceivers', *IEEE Trans. Commun.*, 1996, **44**, (10), pp. 1234–1238
[28] Van Eetvelt, P., Wade, G., Tomlinson, M.: 'Peak to average power reduction for OFDM schemes by selective scrambling', *Electron. Lett.*, 1996, **32**, (21), pp. 1963–1964
[29] Bauml, R., Fischer, R., Huber, J.: 'Reducing the peak-to-average power ratio of multicarrier modulation by selected mapping', *Electron. Lett.*, 1996, **32**, (22), pp. 2056–2057
[30] Simon, M.K., Annavajjala, R.: 'On the optimality of bit detection of certain digital modulations', *IEEE Trans. Commun.*, 2005, **53**, (2), pp. 299–307
[31] Proakis, J.G., Salehi, M.: '*Digital communications*' (McGraw-Hill, New York, NY, USA, 2008, 5th edn.)